

SUPERGENE ORIGIN OF THE LASTARRIA KAOLIN DEPOSIT, SOUTH-CENTRAL CHILE, AND PALEOCLIMATIC IMPLICATIONS

H. A. GILG,¹ S. HÜLMEYER,² H. MILLER,² AND S. M. F. SHEPPARD³

¹ Lehrstuhl für Angewandte Mineralogie und Geochemie, Technische Universität München, Lichtenbergstr. 4, 85747 Garching, Germany

² Institut für Allgemeine und Angewandte Geologie, Ludwig-Maximilians-Universität München, Luisenstr. 37, 80333 München, Germany

³ Laboratoire de Science de la Terre and CNRS-UMR 5570, Ecole Normale Supérieure de Lyon, 46 Allée d'Italie, 69364 Lyon, France

Abstract—The residual kaolin deposits near Lastarria, South-Central Chile, were formed by weathering of subvolcanic quartz porphyry stocks, which intruded the metamorphic basement of the Coastal Cordillera. The clay fractions (<2 µm) consist mainly of poorly-ordered, very fine-grained kaolinite and lath-shaped illite (17–38 wt. %) with minor amounts of quartz, sanidine, and goethite. A sample from the top of the deposit contains major quantities of gibbsite morphologically indistinguishable from kaolinite flakes. The gibbsite-free clays contain 35.5–36.6 wt. % Al₂O₃, 0.4–2.6 wt. % Fe₂O₃, 1.3–3.9 wt. % K₂O, and have low TiO₂ concentrations (<0.02 wt. %). The absence of quartz veining, the abundance of melt inclusions, and the scarcity of secondary fluid inclusions in quartz phenocrysts from altered rocks imply a lack of significant hydrothermal activity in the quartz porphyries. The δ¹⁸O and δD values of the kaolins indicate formation in a weathering environment at significantly higher annual mean air temperatures (~12°C) than present mean temperatures of ~9.4°C. Uplift of the region alone probably cannot account for the change in climate. The stable isotope composition of gibbsite is consistent with an origin of desilication of kaolinite at superficial temperatures. Various criteria proposed to distinguish supergene from hypogene kaolins are discussed.

Key Words—Chemistry, DTA, Fluid Inclusions, Gibbsite, Hydrogen Isotopes, Hydrothermal, Illite, Kaolinite, Origin of Kaolin, Oxygen Isotopes, Weathering.

INTRODUCTION

Primary kaolin deposits may form *in situ* from aluminosilicate rocks by weathering (supergene kaolins), by hydrothermal activity (hypogene kaolins), or in some cases by a combination of the two processes (e.g., Murray, 1988; Murray and Keller, 1993). The origin of many kaolin deposits is, however, controversial. Several methods were proposed or discussed to distinguish between supergene and hypogene kaolins, including the general geological setting, structural setting, mineralogical composition and zoning (e.g., Konta, 1969; Kitagawa and Köster, 1991; Dill *et al.*, 1997), microtextures of the clays (Keller, 1976a, 1976b, 1978), chemical composition (Köster, 1969; Dill *et al.*, 1997), fluid inclusions (Konta, 1969; Manning, 1995), and stable isotope geochemistry (Sheppard *et al.*, 1969; Sheppard, 1977; Marumo *et al.*, 1982; Sheppard and Gilg, 1996).

This study presents the first mineralogical, geochemical, and stable isotope data on the Lastarria kaolin deposit in South-Central Chile. This deposit is one of the southern-most kaolin deposits of the world, together with those of the Chubut and Santa Cruz area, Argentina (Murray, 1988). All these deposits, including Lastarria, are hosted by volcanic or subvolcanic felsic rocks. The genesis of the Patagonian deposits is still a matter of debate; both hydrothermal (Hayase, 1969; Iñiguez Rodríguez, 1982) and weathering ori-

gins (Romero *et al.*, 1974; Murray, 1988; Cravero *et al.*, 1991; Domínguez and Murray, 1995) were proposed. We will provide evidence herein for a supergene origin of the Chilean Lastarria kaolin deposit and discuss the validity of the various criteria proposed to distinguish between supergene and hypogene kaolins. We also address possible paleoclimatic implications derived from our isotope data.

GEOLOGICAL SETTING

Lastarria, near Gorbea, is situated approximately 730 km south of Santiago de Chile on the old Panamerican highway between Temuco and Valdivia in the Araucanía region, south-central Chile (Figure 1). The kaolin deposits are located 8–9 km west of Lastarria. They are presently exploited in two open pits, the very small pit I (39°14'30"S/72°44'00"W; 440–450 m above sea level [a.s.l.]) with a diameter of <100 m and the larger pit II, named Afquintue (39°14'40"S/72°44'30"W; 305–360 m a.s.l.), with a diameter of ~600 m (Figure 2).

The residual kaolins formed on two mushroom-shaped, subvolcanic quartz porphyry stocks which crosscut the low-grade metamorphic basement of the Coastal Cordillera of the Chilean Andes. The crystalline basement near Lastarria transects as a block the main N-S trending Central Valley containing Tertiary to Quaternary sediments including Miocene limno-flu-

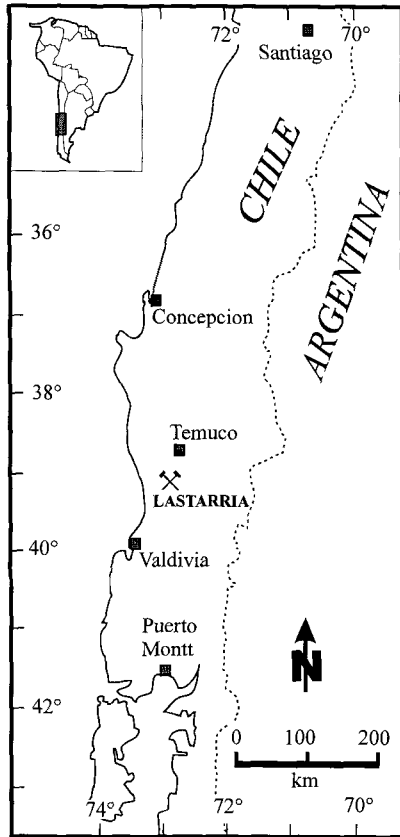


Figure 1. Location map of the Lastarria kaolin deposit, South-Central Chile.

viatil coal measures. Since Miocene times, this basement block was a morphological high as evidenced by wedging-out of clastic sediments in the surrounding basins towards that block. The basement rocks are predominately graphite-bearing mica schists which represent a flyschoid series in an accreted Paleozoic ensialic marginal basin (Hervé *et al.*, 1990; Schira, 1991; Hufmann *et al.*, 1997a, 1997b). The quartz porphyries clearly postdate the Carboniferous low-grade metamorphism of the host rocks (Schira, 1991). Absolute-age data for the igneous activity do not exist, but most probably the quartz porphyry stocks belong to the common Tertiary volcanism which was dated as Late Oligocene to Miocene by Muñoz *et al.* (1997).

Only strongly altered porphyries were observed. In contrast, the metamorphic host rocks, which are devoid of hydrothermal quartz veins, exhibit only very weak kaolinization. At the rims of the open pit II, virtually unaltered mica schists overlie completely kaolinized quartz porphyries (Figure 2). Quartz veins are not present in the porphyries, and therefore are absent from the clay pits.

The mines are owned by *Fábrica Nacional de Loza* (FANALOZA), Penco, Chile. Mining activity occurs only sporadically, and production data are not avail-



Figure 2. Lastarria open pit II (Afquintue) showing a white kaolinized quartz porphyry stock overlain by unaltered graphite-bearing micaschists.

able. However, the material is primarily being used for porcelain manufacture.

MATERIALS AND METHODS

Between December 1995 and March 1996, two representative kaolin samples (IA and IB) were collected from the smaller open pit I and six samples (IIA to IIF) from the larger open pit II. Sample IIE comes from the highest elevation in pit II (370 m a.s.l.), whereas sample IIF from the deepest part (305 m a.s.l.). The other samples come from intermediate positions within pit II. For detail see Table 1.

The $<2 \mu\text{m}$ fraction of each sample was obtained by settling in an aqueous sodium pyrophosphate suspension. The mineralogical composition of the samples was determined using X-ray diffraction (XRD) analysis of oriented and partly glycolated clay mineral aggregate samples (Siemens D500, $\text{CuK}\alpha$ radiation), scanning electron microscopy (SEM) (JEOL 35C) with an energy-dispersive X-ray analyzer, and differential thermal analysis (DTA) (Netsch STA 409C; heating rate: $10^\circ\text{K min}^{-1}$. In air, reference material: Al_2O_3). Major chemical constituents and trace elements of five selected samples ($<2 \mu\text{m}$ fractions of IB, IIA, IIC, IIE, IIF) were determined by X-ray fluorescence analysis (XRF) (Siemens SRS30).

Isotope geochemical studies were conducted at Lehrstuhl für Angewandte Mineralogie und Geochemie, TU München and Laboratoire de Sciences de la Terre, ENS de Lyon. Adsorbed and loosely bound water was removed by heating the samples at 180°C for at least two hours in vacuum. Oxygen was extracted using bromine pentafluoride at $\sim 560^\circ\text{C}$ overnight and converted to carbon dioxide over hot graphite (Clayton and Mayeda, 1963). Hydrogen was extracted by dehydration at $>1500^\circ\text{C}$ and by reduction over hot uranium according to Bigeleisen *et al.* (1952). Isotopic measurements were performed on a VG Prism mass spectrometer. All $\delta^{18}\text{O}$ and δD values are reported in

Table 1. Sample location and mineral composition of Lastarria kaolins (<2 μm fraction).

Sample number	Altitude (m above sea level)	Position within the pit	Mineral composition (wt. %)
Open pit 1: 39°14'30"S; 72°44'00"W			
IA	455	1 m below top of intrusion	—
IB	455	2.5 m below contact	K(60) I(40) Q(<5)
open pit 2: 39°14'40"S; 72°44'30"W ("Afquintue")			
IIA	310	2 m below top of intrusion	K(80) I(15) Q(<5)
IIB	350	at contact to mica schist	—
IIC	360	4 m below surface	K(75) I(25) Goe(<5) Q(<5)
IID	360	1 m above base of intrusion	—
IIE	370	3 m below top of intrusion	K(20) I(40) Gib(40) Q(<5)
IIF	305	central part of intrusion	K(70) I(20) San(<5) Q(<5)

K = kaolinite, I = illite, Q = quartz, Goe = goethite, Gib = gibbsite, San = sanidin.

per mil relative to standard mean ocean water (SMOW). Analytical precision is estimated at <0.3 per mil for oxygen and <2 per mil for hydrogen.

Idiomorphic quartz phenocrysts, with an average diameter of 1 mm, were separated from the >63 μm fraction of the kaolinized porphyry sample IB, embedded in resin and doubly polished for inspection for fluid and melt inclusions.

MINERALOGICAL COMPOSITION

The clay size fractions (<2 μm) of the analyzed samples consist mainly of kaolinite with minor

amounts of illite and quartz (Table 1). Additional constituents detected by XRD are gibbsite in sample IIE, goethite in sample IIC, and K-feldspar in sample IIF. Analyses by XRD, DTA and SEM reveal no evidence for the presence of halloysite in the clays.

Lastarria kaolinite reveals high $d(001)$ values of 7.14–7.30 Å and relatively low intensities for $d(hkl)$ with $k = 3n$ indicating poor crystallinity and abundant layer stacking imperfections. The latter are confirmed by low dehydroxylation temperatures 536–556°C (Figure 3). Kaolinite forms irregular, usually very small (often <2 μm) flakes (Figure 4a). Thick "booklets" or stacks of kaolinite were not found under SEM.

A non-expandable dioctahedral aluminum-rich potassic 10 Å clay mica mineral ("illite") is present in all investigated samples. Its morphology is characterized by very thin (<0.2 μm), but long (up to 4 μm) laths (Figure 4f). The clay mica form "beards" on strongly delaminated K-feldspar phenocrysts (Figures 4c–e).

The presence of gibbsite in one sample (IIE) with the highest elevation in open pit II is confirmed by XRD and DTA. The characteristic endothermic DTA peak near 290°C (Figure 3) is slightly lower than the value of 320–330°C given by MacKenzie (1957). However, quite variable endothermic peak positions of gibbsite from lateritic horizons in Taiwan (280–340°C) were described by Chen *et al.* (1988). The lower values were typical for the uppermost parts of the weathering profiles. The inspection by SEM shows that gibbsite in sample IIE is morphologically indistinguishable from the small kaolinite flakes (Figure 4b).

Residual minerals from the altered quartz porphyries, which are now present in the <2 μm fractions, are quartz, goethite and, in sample IIF, very small amounts of K-feldspar.

INCLUSIONS IN QUARTZ PHENOCRYSTS

The inspection of doubly polished sections of quartz phenocrysts from the altered quartz porphyry reveals the presence of abundant primary silicate-melt inclusions in the cores and in planes of secondary origin

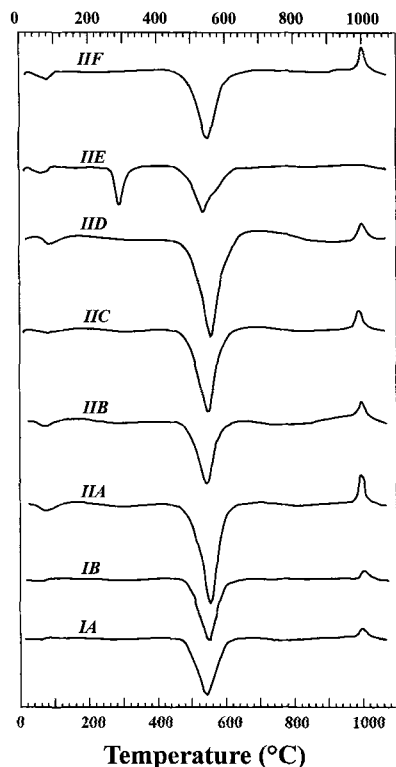


Figure 3. DTA curves of Lastarria kaolins (<2 μm fraction). Note prominent endothermic peak at $\sim 300^\circ\text{C}$ of the gibbsite-bearing sample IIE.

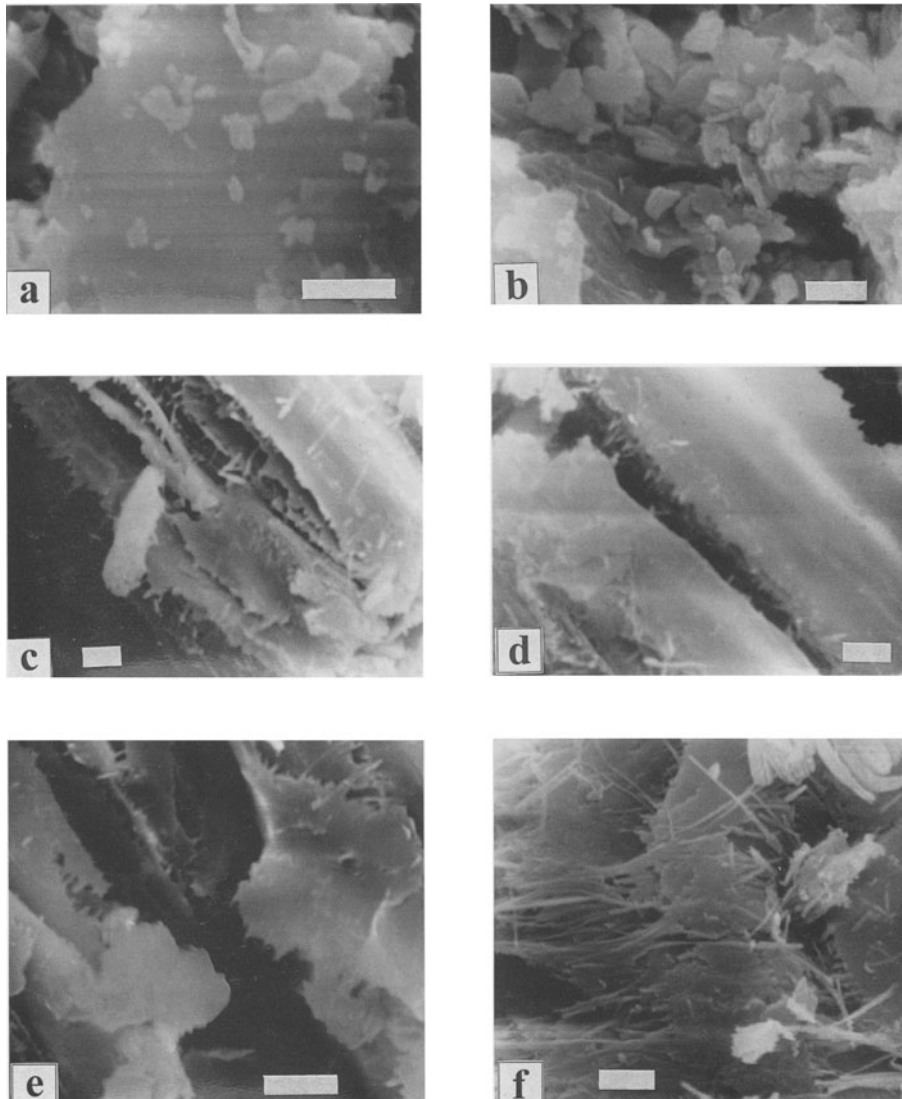


Figure 4. Scanning electron micrographs of kaolins from Lastarria. a) fine-grained anhedral kaolinite flakes (sample IIE). b) kaolinite and gibbsite flakes (sample IIE). c)–f) lath-shaped clay mica mineral (“illite”) growing on delaminated K-feldspar (sample IIC). Scale bars in all micrographs = 2 μm .

(Figures 5a–c). These silicate-melt inclusions represent crystallized inclusions of small melt droplets from the magma.

Secondary aqueous liquid-vapor inclusions formed from healed fractures were observed in less than half of the quartz phenocrysts examined. Such inclusions are not abundant; some are related to large decrepitated melt inclusions. Secondary inclusions are generally rich in aqueous liquid, *i.e.*, they have a high degree of fill ($\text{Vol}_{\text{LIQ}}/(\text{Vol}_{\text{LIQ}} + \text{Vol}_{\text{VAP}})$), and often display necking-down textures. Solid inclusions of kaolinite or illite were not found in the secondary fluid inclusions or in the healed fractures. Secondary trails of vapor-rich two-phase inclusions are also not present in the quartz phenocrysts.

CHEMICAL COMPOSITION

Chemical analyses of selected $<2 \mu\text{m}$ fractions are shown in Table 2. The gibbsite-free kaolins contain 35.5–36.6 wt. % Al_2O_3 , whereas the gibbsite-bearing sample has 45.8 wt. % Al_2O_3 . The Fe_2O_3 concentrations of the clays are variable between 0.41 (IB) and 2.56 wt. % (IIC). Iron-rich samples clearly show a faint orange tint. The TiO_2 contents are very low (<0.02 wt. %). The presence of illite in all samples results in K_2O contents of 1.3–3.9 wt. %. Trace element concentrations of the Lastarria kaolins are within the range reported for other kaolins (Köster, 1969).

Using the chemical data (major oxides) and XRD patterns of the clays, we semiquantitatively estimated

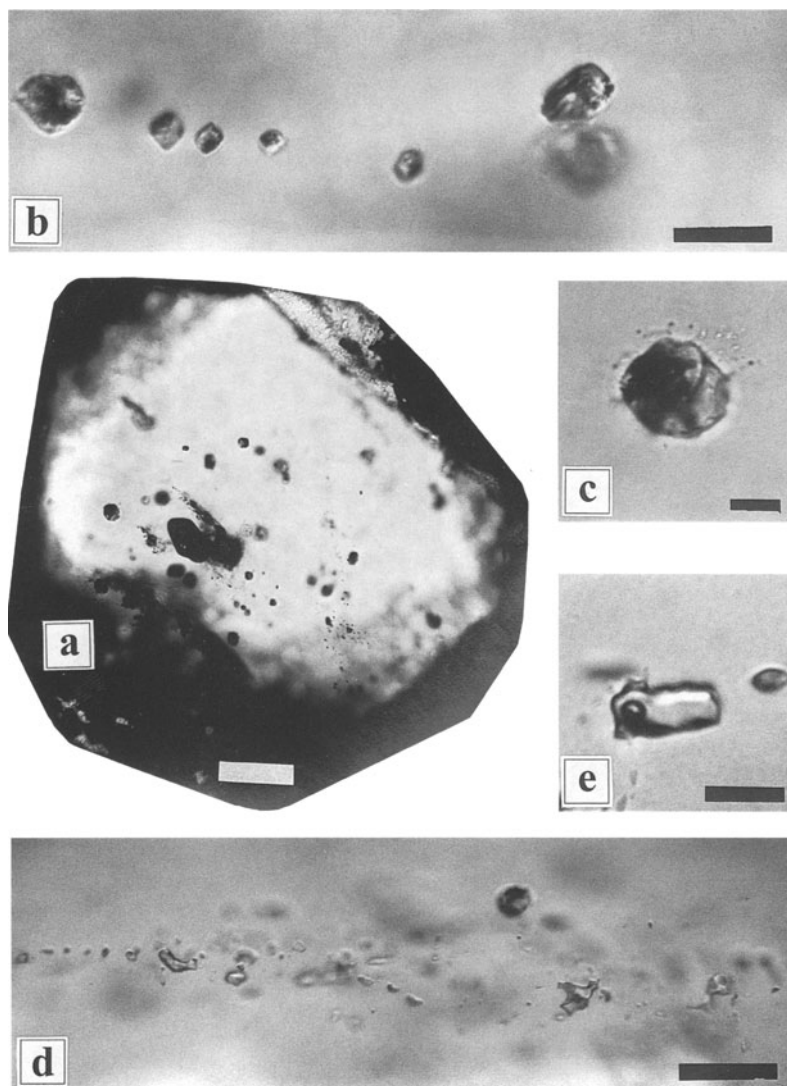


Figure 5. Micrographs of inclusion in quartz phenocrysts from kaolinized quartz porphyry (sample IB) from Lastarria. a) typical random distribution of primary melt inclusions. Note the absence of secondary fluid inclusion trails. Scale bar = 100 μm . b) trail of secondary, crystallized melt inclusions. Scale bar = 20 μm . c) crystallized melt inclusion with halo of small fluid inclusions indicating natural decrepitation. Scale bar = 10 μm . d) trail of secondary liquid-rich two phase fluid inclusions. Scale bar = 40 μm . e) liquid-rich two phase fluid inclusion. Scale bar = 10 μm .

modal compositions. We used the ideal compositions of kaolinite ($\text{Al}_2[\text{Si}_2\text{O}_5(\text{OH})_4]$), quartz (SiO_2), gibbsite ($\text{Al}(\text{OH})_3$), goethite (FeOOH), K-feldspar (KAlSi_3O_8), and an "illite" ($\text{K}_{0.70}\text{Al}_{2.53}\text{Fe}_{0.15}\text{Mg}_{0.02}\text{Si}_{3.30}\text{O}_{10}(\text{OH})_2$). The results are reported in Table 1.

STABLE HYDROGEN AND OXYGEN ISOTOPE DATA

The stable hydrogen and oxygen isotope data of selected clay samples (<2 μm fractions) are presented in Table 3 and plotted in Figure 6. The $\delta^{18}\text{O}$ values of gibbsite-free clays (IB, IIA, IIC, and IIF) vary between 18.2–19.3‰, δD values between -69 and -74‰. There is no systematic variation between δD values

and illite content indicating very similar hydrogen isotope compositions of kaolinite and illite ($\sim -72 \pm 3\%$). The high goethite content of sample IIC explains its relatively low $\delta^{18}\text{O}$ value. Iron oxide hydroxides have much smaller oxygen fractionations between mineral and water than kaolinite or illite (Yapp, 1987; Sheppard and Gilg, 1996). For the other samples, illite contents and $\delta^{18}\text{O}$ values of kaolins are strongly correlated ($r = 0.9$). This relationship allows an estimate of the oxygen isotopic compositions of the pure end-members, kaolinite ($21 \pm 1\%$) and illite ($14 \pm 3\%$). We estimated a much larger error for pure illite because illite contents never exceed 35 wt. %. The <2 μm fractions, as well as the calculated pure kaolinite,

Table 2. Geochemical composition of Lastarria kaolins (<2 μm fraction).

Sample	I B	II A	II C	II E	II F	Detection limit
Major constituents (wt. %)						
SiO ₂	48.60	48.10	46.90	30.10	48.90	0.03
TiO ₂	0.02	0.02	0.03	0.01	0.01	0.003
Al ₂ O ₃	36.50	36.59	36.09	45.80	35.50	0.06
Fe ₂ O ₃	0.41	0.66	2.56	1.86	0.49	0.03
MnO	b.d.l.	b.d.l.	0.02	0.04	b.d.l.	0.002
MgO	0.09	0.05	0.12	0.07	b.d.l.	0.03
CaO	0.18	0.16	0.12	0.14	0.17	0.03
Na ₂ O	0.14	0.08	0.08	0.00	b.d.l.	0.06
K ₂ O	3.90	1.31	2.02	2.87	2.50	0.03
P ₂ O ₅	b.d.l.	0.11	0.04	0.09	0.06	0.02
LOI	11.0	13.3	12.9	19.0	12.5	
Sum	100.84	100.38	100.88	99.98	100.18	
Trace element concentrations (ppm)						
Ba	262	246	255	251	483	60
Co	111	49	83	36	11	24
Cr	132	156	207	146	257	18
Ga	34	28	21	b.d.l.	12	12
Nd	104	92	107	b.d.l.	b.d.l.	90
Ni	120	111	131	99	102	18
Pb	b.d.l.	46	b.d.l.	b.d.l.	b.d.l.	30
Rb	114	51	78	102	76	12
Sr	131	56	65	39	47	12
Th	50	b.d.l.	54	b.d.l.	b.d.l.	12
V	26	b.d.l.	b.d.l.	29	19	18
Y	46	20	58	26	79	12
Zn	58	35	67	65	48	18
Zr	47	79	127	15	27	12

LOI = loss on ignition; b.d.l. = below detection limit.

plot very close to the kaolinite line (Figure 6) defining the isotopic variations of supergene kaolinites (Savin and Epstein, 1970; Sheppard and Gilg, 1996). Waters on the meteoric water line ($\delta\text{D} = 8 \delta^{18}\text{O} + 10$) are in equilibrium with the pure Lastarria kaolinite at temperatures $\sim 15^\circ\text{C}$ (Gilg and Sheppard, 1996; Sheppard and Gilg, 1996). Their δD values are approximately -39‰ . The gibbsite-bearing sample IIE has a low $\delta^{18}\text{O}$ (15.1‰) and high δD value (-55‰). The stable isotope values for the pure gibbsite in this sample calculated by mass balance are $13 \pm 2\text{‰}$ ($\delta^{18}\text{O}$) and $-45 \pm 5\text{‰}$ (δD). The Lastarria gibbsite plots in the $\delta^{18}\text{O}$ — δD diagram (Figure 6) between the two gibbsite lines defining the isotopic variations of supergene gibbsite as proposed by Lawrence and Taylor (1971) and Bird *et al.* (1989).

SUPERGENE VERSUS HYPOGENE KAOLINIZATION AT LASTARRIA

Although the geological position of the Lastarria deposit in subvolcanic quartz porphyry stocks would potentially be favorable for hydrothermal kaolinization, the observations and data presented above clearly support a supergene (weathering) origin and additionally

Table 3. Oxygen and hydrogen isotope analyses from Lastarria.

Sample	$\delta\text{D}_{\text{SMOW}}$ (‰)	$\delta^{18}\text{O}_{\text{SMOW}}$
Kaolins (<2 μm)		
IB	-74.3 ± 1.6 (2)	18.2
IIA	-74.6	19.3
IIC	-74.3	18.4
IIE	-54.7 ± 0.8 (2)	15.1
IIF	-69.1 ± 2.0 (2)	19.1
Pure calculated endmembers		
kaolinite	-72 ± 3	21 ± 1
illite	-72 ± 3	14 ± 2
gibbsite	-40 ± 5	13 ± 2

document the absence of hydrothermal activity in the quartz porphyry stocks of Lastarria. Furthermore, our data allow a discussion and critical evaluation of the various criteria proposed to distinguish supergene from hypogene kaolin deposits elsewhere (*e.g.*, Sheppard *et al.*, 1969; Konta, 1969, 1970; Keller, 1970; Walker, 1970; Bristow, 1977; Bray and Spooner, 1983; Kitagawa and Köster, 1991; Sheppard and Gilg, 1996; Dill *et al.*, 1997).

Mineralogical composition and zoning

Hydrothermal kaolinites are often associated with high-temperature ($>40^\circ\text{C}$) alteration minerals, such as

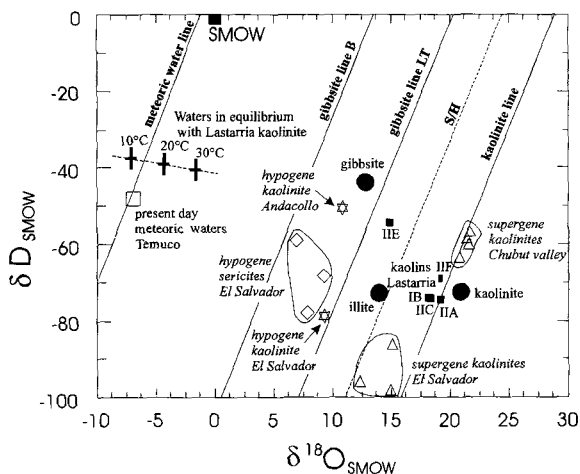


Figure 6. δD versus $\delta^{18}\text{O}$ diagram of Lastarria kaolins (black squares), calculated pure minerals (black dots) and waters in equilibrium with kaolinite (crosses) at temperatures between 10 – 30°C . The kaolinite line modified by Sheppard and Gilg (1996) after Savin and Epstein (1970), the gibbsite lines after Lawrence and Taylor (1971) [LT] and Bird *et al.* (1989) [B] and the line separating hypogene from supergene kaolinites [S/H] from Sheppard *et al.* (1969) are given for reference. Isotopic compositions of supergene and hypogene clay minerals from El Salvador porphyry copper deposit, Chile (Sheppard and Gustafson, 1976), Andacollo Pb-Zn deposit, Neuquén, (Domínguez, 1990), Chubut river valley kaolin deposits, Patagonia, (Cravero *et al.*, 1991) both Argentina and present day meteoric waters from the nearby IAEA station at Temuco, Chile, are shown for comparison.

pyrophyllite, diaspor, dickite, nacrite, topaz, or zunyite, *etc.* (e.g., Keller, 1969; Lombardi and Sheppard, 1977; Marumo, 1989; Reyes, 1991; Arribas *et al.*, 1995; Dill *et al.*, 1997). Other common minerals found in hydrothermal kaolins are illite, illite-smectite mixed-layer minerals, cristobalite, alunite, and complex phosphate-sulfate minerals (e.g., crandallite, svanbergite, woodhouseite, goyazite, *etc.*). However, these latter minerals are also found in weathering environments or superficial oxidation zones and thus are not considered here as diagnostic for a hydrothermal origin. Note, however, that high-temperature minerals from earlier hydrothermal activity, which may or may not be related to kaolinization, can occur as residual minerals in a much later superimposed weathering or oxidation zone (e.g., Konta, 1969; Schoen *et al.*, 1974; Sheppard, 1977). Gibbsite generally does not occur in hydrothermal kaolins and is typical for weathering kaolins.

Additionally, hydrothermal kaolins show a characteristic mineralogical zonation with a kaolinite \pm alunite \pm pyrophyllite zone in the center and an outer illite-smectite-rich zone (Kitagawa and Köster, 1991; Reyes, 1991; Hedenquist *et al.*, 1996). Such a zoning is generally not present in supergene kaolin deposits.

The presence of gibbsite and the absence of high-temperature minerals such as pyrophyllite, diaspor, dickite, or nacrite at Lastarria clearly favor a supergene origin of the kaolins.

Textures of clays

Studying scanning electron micrographs of various clays, Keller (1976a, 1976b, 1978) suggested that kaolins of different origins have characteristic textures. For example, kaolins of hydrothermal origin are typically very fine-grained, tightly packed, and thus have a low porosity. The kaolinite plates occur as singles, sheaves, or thin packets; large kaolinite booklets are not present. Although these features match the textures of Lastarria kaolins, Keller (1976a, 1976b, 1978) also noted that kaolins formed by *in situ* weathering can be very fine-textured if the igneous parent rocks are fine-textured, such as the matrix of quartz porphyries. Thus, clay textures are not an unambiguous means to distinguish kaolins formed by hydrothermal processes from kaolins formed by weathering.

Fluid inclusions

The abundance of fluid inclusions in quartz from kaolinized granites was regarded by Nicolas (1958) as an indicator of hydrothermal kaolinization. However, Konta (1969) found identical fluid-inclusion assemblages in fresh and kaolinized granites from the Karlovy Vary area, Czech Republic, and concluded that fluid inclusions existed in quartz prior to kaolinization. He further suggested that the presence of abundant flu-

id inclusions in quartz cannot be regarded as unequivocal proof of hydrothermal kaolinization.

Contrasting conclusions were drawn by Bray and Spooner (1983) and Alderton and Rankin (1983) in their studies of the Cornish deposits, SW England. Bray and Spooner (1983) found a positive correlation between the degree of kaolinization and the intensity of quartz veining, as well as the abundance of fluid inclusions in quartz at Goonbarrow china clay pit. They suggested that kaolinization involved a high-temperature vapor phase. Alderton and Rankin (1983) could show that the intensity of kaolinization in the St. Austell granite can be correlated with the abundance of low-salinity low-temperature (<170°C) liquid-rich fluid inclusions. It is noted, however, that zones of intensive hypogene kaolinization ("advanced argillic alteration") in active geothermal systems—modern analogs of ancient hypogene kaolin deposits—are generally related to areas of enhanced permeability where the interaction of ascending sulfur- and/or HCl-rich hot magmatic vapors with cold ground waters to produce steam-heated acid fluids (Meyer and Hemley, 1967; Reyes, 1991; Hedenquist *et al.*, 1996). These acid alteration zones are characterized by the abundance of vapor-rich fluid inclusions (Reyes, 1991).

Konta (1969), Sheppard (1977) and Bristow (1977) suggested that hydrothermal alteration in some granite-hosted kaolin deposits was not directly responsible for the main kaolinization, but caused sericitization and increased the permeability of the rocks for later deep weathering.

The scarcity of secondary fluid inclusions in quartz phenocrysts of the kaolinized Lastarria porphyries and the lack of quartz veining in the deposit indicate that there was no strong hydrothermal activity at Lastarria.

Chemical composition

In a recent study, Dill *et al.* (1997) found that some trace elements, e.g., P, Ti, Cr, Nb, Ce, La, and Y, can be used to distinguish between hydrothermal and weathering kaolins from northwestern Peru. If their suggested criteria were applied to the Lastarria deposit, the low-phosphorus and high-chromium plus niobium contents of the Lastarria kaolins would imply a supergene origin, whereas their low-cerium plus lanthanum plus yttrium and low-titanium concentrations would favor a hypogene origin. The criteria of Dill *et al.* (1997) thus cannot be transferred to classify other deposits. For example, the kaolins from Schwertberg (Austria), Hirschau, Tirschenreuth, or Kemmlitz (Germany) of weathering origin have low TiO₂ contents (Köster, 1969) and would thus fall into the field of hydrothermal kaolins of Dill *et al.* (1997). This indicates that trace element compositions of residual kaolins do not only reflect their temperatures of formation, but also strongly depend on the chemical composition of the parent rocks. It is noted that Köster

(1969) did not find any significant differences in trace element concentrations between supergene and hypogene kaolins.

Isotope geochemistry

The use of stable oxygen and hydrogen isotopes to discriminate supergene from hypogene kaolins has been demonstrated by Sheppard *et al.* (1969) and by Marumo *et al.* (1982). In a δD — $\delta^{18}O$ -diagram, kaolinites of weathering origin scatter around the kaolinite line, which presents the isotopic compositions of kaolinites in equilibrium with meteoric waters at 20°C, whereas hydrothermal kaolinites typically plot left to the S/H (supergene/hypogene) line of Sheppard *et al.* (1969). The validity of this approach was confirmed recently by a critical review of Sheppard and Gilg (1996). The kaolins from Lastarria (with the exception of the gibbsite-rich sample IIE), as well as the calculated pure kaolinite, plot very close to the kaolinite line indicating a weathering origin of the clays.

Similarly, the calculated isotopic composition of pure gibbsite plots between the two proposed gibbsite lines of Lawrence and Taylor (1971) and Bird *et al.* (1989), closer to the former one. Bird *et al.* (1994) attributed the discrepancy between the two calibrations primarily to variations in oxygen isotope fractionation between gibbsite and water, which depends not only on temperature, but also on the mechanism of gibbsite formation. Gibbsite formed by desilication of kaolinite should plot near the Lawrence and Taylor line, whereas gibbsite crystallized from a gel or solution, as in most kaolinite-poor bauxite deposits, should plot near the gibbsite line of Bird *et al.* (1989). The stable isotope composition and morphology of gibbsite and its occurrence in a kaolin deposit favors the formation of Lastarria gibbsite by desilication.

Hydrogen and oxygen isotope fractionation factors between illites and water at ambient temperatures are not well known, but extrapolations from higher temperatures suggest similar δD values and $\delta^{18}O$ values are a few per mil smaller compared to kaolinite (Sheppard and Gilg, 1996). Thus, illites in equilibrium with meteoric waters at 20°C should plot close to the S/H-kaolinite of Sheppard *et al.* (1969). The isotopic composition of pure illite from Lastarria is thus consistent with a weathering origin. Note that hydrothermal kaolinites and sericites from the El Salvador porphyry copper deposit, Northern Chile, (Sheppard and Gustafson, 1976) and hypogene kaolinite from the Andacollo Pb-Zn deposit, Neuquén, Argentina (Domínguez, 1990), 300 km to the NE of Lastarria, have much lower $\delta^{18}O$ values compared to kaolinites and illites from Lastarria (Figure 6).

PALEOCLIMATIC IMPLICATIONS

The H- and O-isotope compositions of meteoric waters, and therefore supergene clays, are determined by

climatic factors of which annual mean air temperature is by far the principal variable outside of tropical island and monsoon climates (Rozanski *et al.*, 1993). We can therefore compare the climate during kaolinization with that of the present by determining changes in the isotopic composition of the meteoric waters.

The H- and O-isotope compositions of meteoric waters during kaolinization are calculated from the isotopic compositions of the kaolinite using the point of intersection of the meteoric water line ($\delta D = 8 \delta^{18}O + 10$) with the curve for waters in equilibrium with this kaolinite (Figure 6; Savin and Epstein, 1970; Sheppard and Gilg, 1996). This gives a meteoric water with $\delta D = \sim -39\text{‰}$ and a temperature of $\sim 15^\circ\text{C}$. The latter is only semi-quantitative because of uncertainties in the precise calibration of the O-isotope fractionation at surface temperatures. Using the Global Network for Isotopes in Precipitation (GNIP) data base for the South Pacific Chilean coastal stations including Chillán, Concepción, La Serena, Puerto Montt, Punta Arenas, Temuco and Valparaíso (IAEA/WMO, 1994), the O- (or H-) isotope composition of the local meteoric water is related to its annual mean air temperature by:

$$\delta^{18}O = 0.674 \times t(^{\circ}\text{C}) - 14.16 \quad (1)$$

This relation is very similar to that derived by Dansgaard (1964) for North Atlantic coastal stations. This is important, demonstrating the universality of his expression to coastal regions both in the northern and southern hemispheres. Equation (1) gives a calculated annual mean air temperature of 10.9°C compared with a measured value of 10.8°C for the IAEA station at Temuco (altitude 114 m; Figure 1), using the local meteoric water value of $\delta D = -48\text{‰}$ (or $\delta^{18}O = -6.8\text{‰}$) from 1988–1991 (IAEA/WMO, 1994). For Lastarria, neither the present annual mean air temperature nor the isotopic composition of local meteoric waters is directly available. Based on the Temuco data, they are estimated in two different ways for an altitude of 350 m. (1) Application of the classic meteorological temperature-altitude relation ($-0.58\text{K}/100\text{ m}$; Heyer, 1993) gives a temperature of 9.4°C. Then, from equation (1) meteoric waters have $\delta D = -53\text{‰}$ and $\delta^{18}O = -7.8\text{‰}$. (2) Most δD values of meteoric waters change with altitude by -1.3 to $-3.2\text{‰}/100\text{ m}$ (Fontes, 1980). Lastarria meteoric waters are calculated to have $\delta D = -54 \pm 3\text{‰}$ at 350 m. These two independent estimates are similar.

The major decrease in the δD value of local meteoric waters from -39 to -54‰ implies a significant evolution in the climate to the present temperate-humid one with up to 2100 mm rainfall (Weischet, 1970). The climate during kaolinization was warmer and probably more humid (Parrish *et al.*, 1982). If the difference in δD between the time of kaolinization and the present at Lastarria is principally due to a change in annual mean air temperature and equation (1) is at

least approximately applicable to coastal regions in past times, then the annual mean air temperature during kaolinization is estimated to be $\sim 12^{\circ}\text{C}$. As the basement block of the Coastal Cordillera, on which the Lastarria kaolin deposit is situated, was a morphological high since Miocene times, the $\sim 2.5^{\circ}\text{C}$ change in annual mean air temperature at Lastarria is probably not just related to a change in altitude at Lastarria from sea level to 350 m during uplift of the Andes since kaolinization.

Weathering kaolins from the Chubut river valley, Argentina, which formed during the Upper Jurassic to Lower Cretaceous at higher latitude ($\sim 43^{\circ}30'\text{S}$) than Lastarria, have significantly heavier hydrogen isotopic compositions ($\delta\text{D} = -57$ to -65‰ ; Cravero *et al.*, 1991; Domínguez and Murray, 1995) compared to Lastarria kaolins, indicating even higher annual mean air temperatures during that period. Southern South America experienced barely any change in paleolatitude after the opening of the South Atlantic (cf. Parrish *et al.*, 1982; Scotese *et al.*, 1988). Thus the documented cooling of continental climate in that region, from Late Jurassic/Early Cretaceous (Chubut) via post-mid-Tertiary (Lastarria) to present day, as indicated by systematic changes of isotopic composition of kaolins or meteoric waters, is most probably related to global cooling (Crowley and North, 1991).

CONCLUSIONS

Mineralogical, stable oxygen and hydrogen isotope, and fluid inclusion data suggest that the residual kaolin deposits near Lastarria, South-Central Chile, formed by weathering of quartz porphyry stocks at slightly higher annual mean air temperatures ($\sim 12^{\circ}\text{C}$) than present day ones ($\sim 9.4^{\circ}\text{C}$). The change in climatic conditions is probably not just related to uplift of the Andes. There is no evidence of significant hydrothermal activity in the subvolcanic rocks, which could be related to a pervasive sericitic alteration prior to kaolinization. Clay mica ("illite"), which constitutes from 17 to 38 wt. % of the $< 2\ \mu\text{m}$ fractions of the clays, formed by alteration of K-feldspar phenocrysts at superficial temperatures. Gibbsite, which occurs in the uppermost part of the deposit and is morphologically indistinguishable from kaolinite flakes, probably formed by desilication of kaolinite.

Geological setting, microtextures, and chemical compositions of kaolins are not considered as unambiguous means to distinguish hydrothermal from weathering kaolins. The presence of some characteristic minerals, such as pyrophyllite, diaspor, or dickite in high temperature or gibbsite in low temperature environments, may yield clues to the origin of a kaolin deposit. However, a combination of hydrothermal and superimposed supergene alteration may cause ambiguity in some cases. The study of fluid inclusions in quartz from altered rocks is a very powerful means to

detect circulation of hydrothermal fluids and to reconstruct the thermal regime of paleohydrothermal systems. However, an unambiguous assignment of one or more fluid-inclusion populations to a hydrothermal-kaolinization event should not only be made on the basis of fluid inclusions alone, but should also include identification and study of paragenesis of accidentally trapped solid inclusions, especially clay minerals, and their correlation with fluid-inclusion assemblages. Combined stable oxygen and hydrogen-isotope studies of kaolinites and associated minerals are considered to date to be the most powerful method to constrain temperatures of kaolinization and thus the origin of kaolin.

ACKNOWLEDGMENTS

We are grateful to R. Beiderbeck for XRF analyses, M. Emery and K. Holzhäuser for technical assistance with isotopic analyses and T. Herzog for help with photographs and SEM work. G. Alfaro guided us to the deposit and gave valuable suggestions. We acknowledge the financial help during field work in Chile by Volkswagen Foundation. The comments of an anonymous reviewer improved our manuscript.

REFERENCES

- Alderton, D.H.M. and Rankin, A.K. (1983) The character and evolution of hydrothermal fluids associated with the kaolinized St. Austell granite, SW England. *Journal of the Geological Society (London)*, **140**, 297–309.
- Arribas, A., Jr., Cunningham, C.G., Rytuba, J.J., Rye, R.O., Kelly, W.C., Podwysocki, M.H., McKee, E.H., and Tosdal, R.M. (1995) Geology, geochronology, fluid inclusions and isotope geochemistry of the Rodalquilar gold alunite deposit, Spain. *Economic Geology*, **90**, 795–822.
- Bigeleisen, J., Perlman, M.L., and Prosser, H.C. (1952) Conversion of hydrogenic materials to hydrogen for isotopic analysis. *Analytical Chemistry*, **24**, 1356–1357.
- Bird, M.I., Chivas, A.R., and Andrew, A.S. (1989) A stable-isotope study of lateritic bauxites. *Geochimica et Cosmochimica Acta*, **53**, 1411–1420.
- Bird, M.I., Longstaffe, F.J., Fyfe, W.S., Tazaki, K., and Chivas, A.R. (1994) Oxygen-isotope fractionation in gibbsite: synthesis experiments versus natural samples. *Geochimica et Cosmochimica Acta*, **58**, 5267–5277.
- Bray, C.J. and Spooner, E.T.C. (1983) Sheeted vein Sn-W mineralization and greisenization associated with economic kaolinization, Goonbarrow china clay pit, St. Austell, Cornwall, England: geologic relationships and geochronology. *Economic Geology*, **78**, 1064–1089.
- Bristow, C.M. (1977) A review of the evidence for the origin of the kaolin deposits in S.W. England. *Proceedings of 8th International Kaolin Symposium and Meeting on Alunite*, Madrid-Rome, 19 pp.
- Chen, C-H., Liu, K-K., and Shieh, Y-N. (1988) Geochemical and isotopic studies of bauxitization in the Tatun volcanic area, northern Taiwan. *Chemical Geology*, **68**, 41–56.
- Clayton, R.N. and Mayeda, T.D. (1963) The use of bromine pentafluoride in the extraction of oxygen from oxides and silicates for analysis. *Geochimica et Cosmochimica Acta*, **27**, 43–52.
- Cravero, F., Domínguez, E. and Murray, H.H. (1991) Valores $\delta^{18}\text{O}$ y δD en caolinitas indicadores de un clima templado-humedo para el Jurásico superior-Cretácico inferior de la Patagonia. *Revista de la Asociación Geológica Argentina*, **46**, 20–25.
- Crowley, T.J. and North, G.R. (1991) *Paleoclimatology*. Oxford University Press, New York, 183–211.

- Dansgaard, W. (1964) Stable isotopes in precipitation. *Tellus*, **16**, 436–468.
- Dill, H.G., Bosse, H.-R., Henning, K.-H., Fricke, A., and Ahrendt, H. (1997) Mineralogical and chemical variations in hypogene and supergene kaolin deposits in a mobile fold belt of the Central Andes of northwestern Peru. *Mineralium Deposita*, **32**, 149–163.
- Domínguez, E. (1990) $\delta^{18}\text{O}$ ‰, $\delta^{34}\text{S}$ ‰, δD ‰ en piritita y caolinita como indicadores de procesos hidrotermales magmáticos en Andacollo, Neuquén. (nota breve). *Revista de la Asociación Geológica Argentina*, **45**, 403–406.
- Domínguez, E. and Murray, H.H. (1995) Genesis of the Chubut river valley kaolin deposits, Argentina, and their industrial applications. In *Clays Controlling the Environment: Proceedings of the 10th International Clay Conference Adelaide, Australia 1993*, G.J. Churchmann, R.W. Fitzpatrick, and R.A. Eggleton, eds., CSIRO Publishing, Melbourne, 129–134.
- Fontes, J.C. (1980) Environmental isotopes in groundwater hydrology. In *Handbook of Environmental Isotope Geochemistry, Volume 1*, P. Fritz and J.C. Fontes, eds., Elsevier, Amsterdam, 179–226.
- Gilg, H.A. and Sheppard, S.M.F. (1996) Hydrogen isotope fractionation between kaolinite and water revisited. *Geochimica et Cosmochimica Acta*, **60**, 529–533.
- Hayase, K. (1969) Génesis del yacimiento de caolín de la mina “Villegas”, provincia de Chubut, República Argentina. *Revista de la Asociación Geológica Argentina*, **24**, 55–71.
- Hedenquist, J.W., Izawa, E., Arribas, A., and White, N.C. (1996) Epithermal gold deposits: styles, characteristics and exploration. *Journal of the Society of Resource Geology Special Publication*, **1**, 1–16.
- Hervé, F., Pankhurst, R.J., Brook, M., Alfaro, G., Frutos, J., Miller, H., Schira, W., and Amstutz, C. (1990) Rb-Sr and Sm-Nd data from some massive sulfide occurrences in the metamorphic basement of South-Central Chile. In *Strata-bound Ore Deposits in the Andes*, L. Fontboté, G.C. Amstutz, M. Cardozo, E. Cedillo, and J. Frutos, eds., Springer Verlag, Berlin, 221–228.
- Heyer, E. (1993) *Witterung und Klima*. B.G. Teubner, Leipzig, 344 pp.
- Hufmann, L., Miller, H., and Alfaro, G. (1997a) Ophiolithabfolge in der südchilenischen Küstenkordillere mit Back-arc Beckensignatur. *Berichte der Deutschen Mineralogischen Gesellschaft, Supplement to European Journal of Mineralogy*, **9**, 166.
- Hufmann, L., Miller, H., and Alfaro, G. (1997b) Ocean floor magmatic rocks within the accretionary belt of Cerros de Maulén area, Coastal Range, IX. región, Chile. VIII Congreso Geológico Chileno Antofagasta Actas, **3**, 1650–1655.
- IAEA/WMO. (1994) *Global Network for Isotopes in Precipitation (GNIP) Database*. IGBP PAGES/World Data Center-A for Paleoclimatology Data Contribution Series # 94-005. NOAA/NGDC Paleoclimatology Program, Boulder, Colorado. (accessible through <http://www/iaea.or.at/programs/ri/gnip/gnipmain.htm>)
- Infúez Rodríguez, A.M. (1982) Basaltic and rhyolitic rocks as parent materials of halloysite in Argentine deposits. *Developments in Sedimentology*, **35**, 605–612.
- Keller, W.D. (1969) Classification and problems of hydrothermal refractory clay deposits in Mexico. In *Proceedings of the International Clay Conference, Tokyo, Volume 1*, L. Heller, ed., Israel University Press, 305–312.
- Keller, W.D. (1970) Discussion of J. Konta: Comparison of the proofs of hydrothermal and supergene kaolinization in two areas of Europe. In *Proceedings of the International Clay Conference, Tokyo, Volume 2*, L. Heller, ed., Israel University Press, 91–93.
- Keller, W.D. (1976a) Scan electron micrographs of kaolins collected from diverse environments of origin—I. *Clays and Clay Minerals*, **24**, 107–113.
- Keller, W.D. (1976b) Scan electron micrographs of kaolins collected from diverse environments of origin—II. *Clays and Clay Minerals*, **24**, 114–117.
- Keller, W.D. (1978) Scan electron micrographs of the kaolinization process including examples from the Bohemian Massif. *Schriftenreihe fuer Geologische Wissenschaften, Berlin*, **11**, 89–108.
- Kitagawa, R. and Köster H.M. (1991) Genesis of the Tirschenreuth kaolin deposit in Germany compared with the Kohdachi kaolin deposit in Japan. *Clay Minerals*, **26**, 61–79.
- Konta, J. (1969) Comparison of the proofs of hydrothermal and supergene kaolinization in two areas of Europe. In *Proceedings of the International Clay Conference, Tokyo, Volume 1*, L. Heller, ed., Israel University Press, 281–290.
- Konta, J. (1970) Discussion of J. Konta: Comparison of the proofs of hydrothermal and supergene kaolinization in two areas of Europe. In *Proceedings of the International Conference, Tokyo, Volume 2*, L. Heller, ed., Israel University Press, 91–93.
- Köster, H.M. (1969) Beitrag zu Geochemie der Kaoline. In *Proceedings of the International Clay Conference, Tokyo, Volume 1*, L. Heller, ed., Israel University Press, 273–280.
- Lawrence, J.R. and Taylor, H.P. (1971) Deuterium and oxygen-18 correlation: Clay minerals and hydroxides in Quaternary soil compared to meteoric waters. *Geochimica et Cosmochimica Acta*, **35**, 993–1003.
- Lombardi, G. and Sheppard, S.M.F. (1977) Petrographic and isotopic studies of the altered acid volcanics of the Tolfa-Cerite area, Italy: The genesis of the clays. *Clay Minerals*, **12**, 147–162.
- MacKenzie, R.C. (1957) *The Differential Thermal Analysis of Clays*. Mineralogical Society, London, 456 pp.
- Manning, D.A.C. (1995) *Introduction to Industrial Minerals*. Chapman & Hall, London, 276 pp.
- Marumo, K. (1989) Genesis of kaolin minerals and pyrophyllite in Kuroko deposits of Japan: Implications for the origin of the hydrothermal fluids from mineralogical and stable isotope data. *Geochimica et Cosmochimica Acta*, **53**, 2915–2924.
- Marumo, K., Matsuhisa, Y., and Nagasawa, K. (1982) Hydrogen and oxygen isotopic composition of kaolin minerals in Japan. *Developments in Sedimentology*, **35**, 315–320.
- Meyer, C. and Hemley, J.J. (1967) Wall rock alteration. In *Geochemistry of Hydrothermal Ore Deposits*, H.L. Barnes, ed., Holt, Rinehart and Winston, New York, 166–235.
- Muñoz, J., Duhart, P., Crignola, P., Farmer, G.L., and Stern, C. (1997) The mid-Tertiary coastal magmatic belt, South-Central Chile. VIII Congreso Geológico Chileno Antofagasta Actas, **3**, 1694–1698.
- Murray, H.H. (1988) Kaolin minerals: Their genesis and occurrences. In *Hydrous phyllosilicates (Reviews in Mineralogy, Volume 19)*, S.W. Bailey, ed., Mineralogical Society of America, Washington, DC, 67–89.
- Murray, H.H. and Keller, W.D. (1993) Kaolins and kaolins. In *Kaolin Genesis and Utilization*, H.H. Murray, W. Bundy, and C. Harvey, eds., The Clay Mineral Society, Boulder, Colorado, 1–24.
- Nicolas, J. (1958) Sur la genèse des kaolins de Guiscriff (Finistère). *Clay Minerals Bulletin*, **3**, 244–248.
- Parrish, J., Ziegler, A., and Scotese, C. (1982) Rainfall patterns and the distribution of coals and evaporites in the Mesozoic and Cenozoic. *Paleogeography Paleoclimatology and Paleoecology*, **40**, 67–101.
- Reyes, A.G. (1991) Mineralogy, distribution and origin of acid alteration in Philippine geothermal systems. *Geologi-*

- cal Survey of Japan, Special Report: Chishitsu Chosasho Tokubetsu Hokoku*, **277**, 59–66.
- Romero, A.J.B., Domínguez, E., and Whewell, R. (1974) *El área caolinera del Departamento de Gaimán, Provincia de Chubut*. Fundación Bariloche, Centro Nacional Patagónico, 423–444.
- Rozanski, K., Araguás-Araguás, L., and Gonfiantini, R. (1993) Isotopic patterns in modern global precipitation. In *Climate Change in Continental Isotopic Records. Geophysical Monograph* 78, P.K. Swart, K.C. Lohmann, J. McKenzie, and S. Savin, eds., American Geophysical Union, Washington, DC, 1–36.
- Savin, S.M. and Epstein, S. (1970) The oxygen and hydrogen isotope geochemistry of clay minerals. *Geochimica et Cosmochimica Acta*, **34**, 25–42.
- Scotese, C., Gahagan, L., and Larson, R. (1988) Plate tectonic reconstruction of the Cretaceous and Cenozoic ocean basins. *Tectonophysics*, **155**, 27–48.
- Schira, W. (1991) *Die Südliche Küstenkordillere Chiles*. Dissertation, University of Heidelberg, Heidelberg, Germany, 238 pp.
- Schoen, R., White, D.E., and Hemley, J.J. (1974) Argillization by descending acid at Steamboat Springs, Nevada. *Clays and Clay Minerals*, **22**, 1–22.
- Sheppard, S.M.F. (1977) The Cornubian batholith, SW England: D/H and $^{18}\text{O}/^{16}\text{O}$ studies of kaolinite and other alteration minerals. *Journal of the Geological Society (London)*, **133**, 573–591.
- Sheppard, S.M.F. and Gilg, H.A. (1996) Stable isotope geochemistry of clay minerals. *Clay Minerals*, **31**, 1–24.
- Sheppard, S.M.F. and Gustafson, L.B. (1976) Oxygen and hydrogen isotopes in the porphyry copper deposit at El Salvador, Chile. *Economic Geology*, **71**, 1549–1559.
- Sheppard, S.M.F., Nielsen, R.L., and Taylor, H.P. (1969) Oxygen and hydrogen isotope ratios of clay minerals from porphyry copper deposits. *Economic Geology*, **64**, 755–777.
- Walker, G.F. (1970) Discussion of J. Konta: Comparison of the proofs of hydrothermal and supergene kaolinization in two areas of Europe. In *Proceedings of the International Clay Conference, Tokyo, Volume 2*, L. Heller, ed., Israel University Press, 91–93.
- Weischet, W. (1970) *Chile, Seine Landeskundliche Individualität und Struktur*. Wissenschaftliche Buchgesellschaft, Darmstadt, 268–365.
- Yapp, C.J. (1987) Oxygen and hydrogen isotope variations among goethites ($\alpha\text{-FeOOH}$) and determination of paleotemperatures. *Geochimica et Cosmochimica Acta*, **51**, 355–364.

(Received 6 November 1997; accepted 15 September 1998; Ms. 97-101)